한국측지학회지, 제 16권, 제 1호, pp.17~26(1998년 6월 30일)

Fast Hartley Transform Technique as a Efficient Tools for Gravity Field Modelling
중력장 모델링을 위한 고속 Hartley 변환기법의 적용

Yun, Hong-Sic*
윤 홍 식

ABSTRACT

This paper deals with gravimetric geoid determination by Fast Hartely transform (FHT) technique in and around the Korean peninsula. A number of data files were compiled for this work, containing now more than 69, 001 point gravity data on land and ocean areas. Especially, regression was applied to estimate gravity anomalies in the northern area of peninsula. For evaluating accuracy of geoid obtained, GPS/Leveling data of 49 stations were prepared. EGM96 global geopotential model to degree 360 was used in order to determine the long wavelength effect of geoid undulations. By applying the remove-restore technique geoid undulations were determined by combining a geopotential model, free-air gravity anomalies. Fast Hartley Transform technique is a suitable solution that uses the advanced spectral technique on the sphere. It was applied to predict geoid undulations by Stokes's integral. Accuracy of geoid undulations was evaluated by comparing with results derived from GPS/Leveling. Standard deviation of differences is about 33 cm.

요 지

본 논문은 Fast Hartley Transform 기법을 소개하고 이를 이용하여 한반도 주변의 지오이드를 결정하기 위한 것이다. 본 연구에서 사용한 중력 측정 데이터는 69,001점으로 남한지역과 BGI로부터 획득한 해상중력데이터로 구성하였으며, 북한쪽은 회기분석에 의하여 1 km×1 km 격자 간격으로 추정하였다. 지오이드의 결정을 위하여 96년에 발표된 EGM96 포텐셜모델을 채택하여 차수 360까지 계산하여 장 파장효과를 구하였고, FHT기법을 적용하여 중력데이터로부터 중 파장효과를 계산하여 이들 두 효과를 합하여 최종 지오이드면을 결정하였다. 본 연구를 통하여 얻어진 지오이드고를 GPS/Leveling에 의하여 구한 지오이드고와 비교한 결과 표준편차가 약 33 cm 이었다.

1. Introduction

With the successful development of the Global Positioning System, geoid determination enjoys a renewed popularity. In many positioning, mapping and exploration applications, conventional sprit leveling is being replaced by orthometric height determination using GPS and the geoid. By using GPS, three-dimensional coordinates or coordinate differences are obtained in a cartesian frame, and the X, Y, Z coordinates obtained are easily convertible into ellipsoidal coordinates-latitude, longitude and height above the ellipsoid. However, the conversion of ellipsoidal height into an orthometric height requires an accurate geoid undulation. The relative accuracy of the gravimetric geoid undulations should meet at least the same accuracy level (see, e. g., Schwarz et at., 1987; Li, 1993),

This means that by combining relative ellipsoidal heights Δh from GPS and relative geoid undulations ΔN, orthometric height differences can be determined ($\Delta H = \Delta h - \Delta N$), provided ΔN is of the same accuracy as Δh. To achieve such accurate

*Lecturer, Department of Civil Engineering, Sungkyunkwan University

results, more advanced methods currently available for gravimetric geoid determination should be used and different data types should be optimally combined (see, e.g., Tziavos, 1993). GPS highlighted the necessity of an accurate geoid model. Especially in order to meet the needs of geodetic leveling, a geoid of centimeter precision level should be provided.

The main goals of this paper are to introduce the Fast Hartley Transform and its application in physical geodesy, and to determine the geoid surface in and around the Korean peninsula using all available surface gravity data, estimated gravity data and a global geopotential model (EGM96). By applying the remove-restore technique, gravimetric geoid undulations were determined.

2. Solutions to the Geodetic Boundary Value Problem

The well-known Stokes formula for the geoid undulations relative to the reference ellipsoid is

$$N = \frac{R}{4\pi\gamma}\iint_{\sigma} \Delta g S(\psi)\, d\sigma \tag{1}$$

where R is mean radius of the earth, and σ denotes the earth's surface. $S(\psi)$ is the Stokes' function and is given by the expression

$$S(\psi) = \operatorname{cosec}\left(\frac{\psi}{2}\right) - 6\sin\left(\frac{\psi}{2}\right) + 1 - 5\cos(\psi) - 3\cos(\psi)\ln\left[\sin\left(\frac{\psi}{2}\right) + \sin^2\left(\frac{\psi}{2}\right)\right] \tag{2}$$

where ψ is the spherical distance between the data and the computation point. For small distances inside an area E, we can use the planar approximation, where the first term of $S(\psi)$ is the dominant one. Thus we have

$$\frac{1}{\sin(\psi/2)} \approx \frac{2}{\psi} \approx \frac{2R}{l} \tag{3}$$

$$R^2 d\sigma = dxdy \tag{4}$$

and equation (1) reduces to

$$N = \frac{1}{2\pi\gamma}\iint_{E} \frac{\Delta g}{l}\, dxdy = \frac{1}{\gamma} S\Delta\sigma \tag{5}$$

$$l = [(x - x_p)^2 + (y - y_p)^2]^{1/2} \tag{6}$$

where (x, y) are the coordinates of the data point and (x_p, y_p) are the coordinates of the computation point and S is Stokes operator.

3. Practical Determination of Geoid

3.1 Pre-processing and Post-processing

The use of Stokes' equation (1) requires gravity anomalies all over the earth for the computation of a single geoid undulation. Obviously, this is impractical to say the least and thus, in practice, some modifications of technique are necessary. If we apply equation (5) instead of equation (1) in a certain region, long wavelength contributions of the gravity field will not be present in results and must be computed in another way. They are provided by a set of spherical harmonic coefficients (geopotential model, GM). Also, due to the density of gravity data, which on the average is no better than $5' \times 5'$, short wavelengths will not be present. They are computed by using topographic heights, which are usually given in the form of a 1km by 1km Digital Terrain Model (DTM). These frequency contributions are shown in Fig. 1.

Computation of geoid undulations N by combining a GM, mean free-air gravity anomalies Δg_{FA}, and heights H in a DTM is based on the following formula (Vanicek and Christou, 1994):

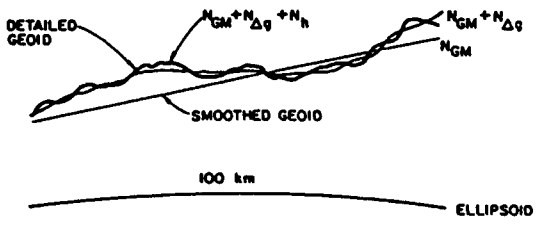

Fig. 1. Contributions of different data to regional geoid determination

$$N = N_{GM} + N_{\Delta g} + N_H \tag{7}$$

$$\Delta g = \Delta g_{GA} - \Delta g_H \tag{8}$$

Although geoid undulations are more sensitive to the low to medium frequencies of the field, in rough topography all the data sets are necessary for estimating N. Note that gravity anomalies used with Stokes' equation have the contributions of the topography and the GM removed. Thus, pre-processing stage involves the computation and removal of the GM and terrain contributions from free-air gravity anomalies and post-processing step involves restoration of the GM contribution and the terrain contribution to N via indirect offset term N_H.

3.2 Computation of the GM-Contributions

Expression for geoid undulations derived from a geopotential model, N_{GM}, takes the following form

$$N_{GM} = \frac{GM}{\gamma}\left\{\sum_{n=2}^{n_{max}}\sum_{m=0}^{n}\left(\frac{a}{r}\right)^n[\bar{C}_{mm}\cos m\lambda + \bar{S}_{mm}\sin m\lambda]\,\bar{P}_{nm}(\sin\phi)\right\} \tag{9}$$

where C_{mm}, S_{nm} are fully normalized harmonic coefficients of the anomalous potential, $\bar{P}_{nm}(\sin\phi)$ are fully normalized Legendre functions, and n_{max} is the maximum degree of geopotential model. Simple application of the so-called fundamental equation of physical geodesy together with Bruns' equation enables sum of the harmonic components of gravity anomalies up to any given degree to be calculated from the same series as geoid undulations, namely

$$\Delta g_{GM} = \frac{GM}{r^2}\left\{\sum_{n=2}^{n_{max}}\sum_{m=0}^{n}(n-1)\left(\frac{a}{r}\right)^n[\bar{C}_{mm}\cos m\lambda + \bar{S}_{mm}\sin m\lambda]\,\bar{P}_{nm}(\sin\phi)\right\} \tag{10}$$

where Δg_{GM} is the total components of gravity anomaly up to degree n_{max}.

For the determination of the long wavelength part of geoid undulations, various geopotential models are available. Tests were carried out to find which of current model is the best to use as a reference model for the Korean peninsula. Com-

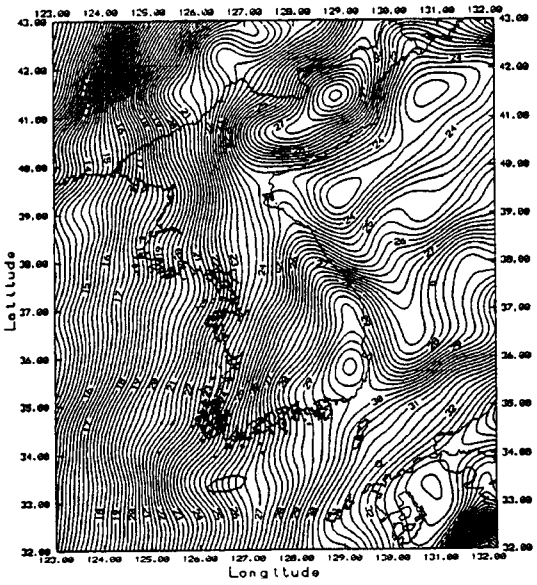

Fig. 2. Geoid Undulation based on the EGM96 geopotential model to degree 360. Contour Interval : 25 cm

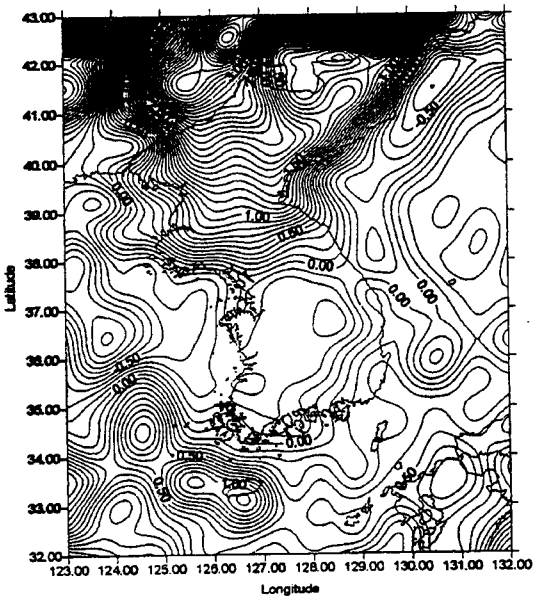

Fig. 3. Differences between gravity anomalies implied by the OSU91A and EGM96 geopotential models. Contour Interval : 1 mGal

parison of solutions with gravity data, GPS data and each models in the Korean peninsula showed that the OSU91A model to degree 360 fit the best (Yun and Adam, 1994, Yun, 1995). New geopotential model (EGM96) announced in Oct. 1996 was tested and compared to the OSU91A. It was shown that there is no large difference between these two models in the southern area of the Korean Peninsula as shown in Fig. 3.

3.3 Computation of the Δg-Contribution

Hartley (1942) proposed the use of a new kind of transform which is expressed in a more symmetrical form between the function of original real variable and its transform, which forms the basis for present discrete formulation. For this reason, it was appropriate to name the Discrete Hartley Transform (DHT) and the Fast Hartley Transform (FHT), which was derived from Hartley's original idea, in his honor (Li and Sideris 1992).

The Hartley transform can also be performed by a fast digital processing, convolution and correlation etc. algorithm. The FHT is as fast as or fast than the FFT and serves for all the uses, such as spectral analysis, to which the FFT is at present applied. In the real and imaginary parts of the Fourier transform or the power spectrum are the desired products, they can be obtained directly from the DHT. Convolution or correlation algorithm can be further simplified if one of functions is even, which is the case usually occurring in physical geodesy, such as the kernels of both planar Stokes' formula and the terrain correction formula.

3.3.1 Definition of the 2-D Continuous Hartley Transform

Hartley (1942) defined a more symmetrical 1-dimensional Fourier transform as follows

$$H(\omega) = \int_{-\infty}^{\infty} h(t)\,\mathrm{cas}\,2\pi\omega t\,dt \tag{11}$$

$$h(t) = \int_{-\infty}^{\infty} H(\omega)\,\mathrm{cas}\,2\pi\omega t\,d\omega \tag{12}$$

where cas x = cos x+sin x.

Because transform pairs (11) and (12) was first defined by Hartley, (11) is called the direct Hartley transform and (12) is called the inverse Hartley transform (Bracewell, 1983 and 1986)

$$H(u, v) = H\{h(x, y)\} = \int_{-\infty}^{\infty}\int_{-\infty}^{\infty} h(x, y)\,\mathrm{casux}\,\mathrm{casvy}\,dxdy \tag{13}$$

$$H(x, y) = H^{-1}\{h(u, v)\} = \frac{1}{4\pi^2}\int_{-\infty}^{\infty}\int_{-\infty}^{\infty} h(u, v)\,\mathrm{casux}\,\mathrm{casvy}\,dudv \tag{14}$$

where H and H^{-1} is the direct and the inverse two dimensional Hartley transform operators.

Let

$$u = 2\pi k_x,\ v = 2\pi k_y \tag{15}$$

and substitute equation (15) into equation (13) and (14) to get

$$H(k_x, k_y) = H\{h(x, y)\} = \int_{-\infty}^{\infty}\int_{-\infty}^{\infty} h(x, y)\,\mathrm{cas}\,2\pi k_x x\,\mathrm{cas}\,2\pi k_y\,dxdy \tag{16}$$

$$h(x, y) = H^{-1}\{H(k_x, k_y)\} = \int_{-\infty}^{\infty}\int_{-\infty}^{\infty} H(k_x, k_y)\,\mathrm{cas}\,2\pi k_x x\,\mathrm{cas}\,2\pi k_y\,dk_x\,dk_y \tag{17}$$

the Hartley transform pair (13) and (14) or (16) and (17) can be simply denoted by

$$h(x, y) <=> H(u, v) \text{ or } h(x, y) <=> H(k_x, k_y) \tag{18}$$

3.3.2 The 2-D Discrete Hartley Transform (2-D DHT)

Here, we can define the Hartley transform of a function given at M×N discrete points on a grid of X and Y coordinates for periods T_x and T_y, the intervals (grid spacings) are given by

$$\Delta x = \frac{T_x}{M},\ \Delta y = \frac{T_y}{M} \tag{19}$$

and the coordinates at node (k, l) are

$$x_k = k\Delta x,\quad k = 0,1,.....,M-1 \tag{20}$$

$$y_l = l\Delta x,\quad l = 0,1,.....,N-1 \tag{21}$$

Let

$$\Delta u = \frac{1}{T_x} \ , \ \Delta v = \frac{1}{T_y} \tag{22}$$

$$u_m = m\Delta u, \ m = 0,1,.....,M-1 \tag{23}$$

$$v_n = n\Delta v, \ n = 0,1,.....,N-1 \tag{24}$$

We can define the two dimensional discrete Hartley transform as

$$H(m\Delta u, n\Delta v) = \Delta x\Delta y \sum_{k=0}^{M-1}\sum_{l=0}^{N-1} h(k\Delta x, l\Delta y)\, cas\frac{2\pi mk}{M}\, cas\frac{2\pi nl}{N} \tag{25}$$

$$h(k\Delta x, l\Delta y) = \frac{1}{T_xT_y}\sum_{m=0}^{M-1}\sum_{nl=0}^{N-1} H(m\Delta u, n\Delta v)\, cas\frac{2\pi mk}{M}\, cas\frac{2\pi nl}{N} \tag{26}$$

For convenience, the DHT pair of equations (25) and (26) is presented using only the integers k, l and m, n as

$$h(k, l) <=> H(m, n) \tag{27}$$

Although the above described definitions are very convenient for the computation of convolution and correlation, they are not suitable for spectral analysis because they have no simple physical interpretation as an oblique wave. In order to study the spectral properties of a function, we could use another kind of kernel, cas[2π(mk/M+nl/N)], instead of cas2πmk /Mcas2πnl/N used in equations (25) and (26) to define the two dimensional discrete Hartley transform as (Bracewell et al., 1986)

$$H(m, n) = \sum_{k=0}^{M-1}\sum_{l=0}^{N-1} h(k, l)\, cas\left(\frac{2\pi mk}{M} + \frac{2\pi nl}{N}\right) \tag{28}$$

$$h(k, l) = \sum_{k=0}^{M-1}\sum_{l=0}^{N-1} H(m, n)\, cas\left(\frac{2\pi mk}{M} + \frac{2\pi nl}{N}\right) \tag{29}$$

However, the kernel cas[2π(mk/M+nl/N)], unlike exp.[-j 2π(mk/M+nl/N)] or that in equations (25) and (26), is not separable into product of factors. So, this kind of transform can not be performed by direct analogy to the two dimensional FFT. To get H(m, n), we should first compute H(m, n) via equation (25), and then evaluate H(m, n) according to the expression 2H(m, n) = H(m, n)+H(-m, n)+H(m,-n)-H(-m,-n).

Because our interest is usually how to compute the convolution efficiently, throughout this paper, we will discuss and use the Hartley transform pair defined by equation (25) and (26). To perform the two dimensional discrete Hartley transform, we transferred a one dimensional basic radix-2 subroutine (Bold, 1985) into Fortran and made some modifications.

3.3.3 The Properties of the 2-D Hartely Transform

The following properties of two dimensional discrete Hartley transform can be derived directly from definitions and, therefore, are listed below without proof. For simplicity, we will write equations (25) and (26) as

$$H(m, n) = \Delta x\Delta y \sum_{k=0}^{M-1}\sum_{l=0}^{N-1} h(k, l)\, cas\, mk\, cas\, nl \tag{30}$$

$$h(k, l) = \frac{1}{T_xT_y}\sum_{k=0}^{M-1}\sum_{l=0}^{N-1} H(m, n)\, cas\, mk\, cas\, nl \tag{31}$$

(a) linearity

$$a\, h(k, l) + b\, g(k, l) <=> a\, H(m, n) + b\, G(m, n) \tag{32}$$

(b) spacing shifting

$$h(k-\lambda, l-\mu) <=> H(m, n)\cos m\lambda\cos n\mu - H(m, -n)\cos m\lambda\sin n\mu - H(-m, n)\sin m\lambda\cos n\mu + H(-m, -n)\sin m\lambda\sin n\mu \tag{33}$$

If λ=M/2 and μ=N/2, then

$$h\left(k-\frac{M}{2}, l-\frac{N}{2}\right) <=> (-1)^{m+n} H(m, n) \tag{34}$$

(c) even function

$$h_e(k, l) <=> H_e(m, n) = \Delta x\Delta y \sum_{k=0}^{M-1}\sum_{l=0}^{N-1} h_e(k, l)\cos mk\cos nl \tag{35}$$

(d) odd function

$h_o(k, l) <=>$

$$H_o(m, n) = \Delta x \Delta y \sum_{k=0}^{M-1} \sum_{l=0}^{N-1} h_o(k, l) \cos mk \cos nl \quad (36)$$

(e) convolution

$$h(k, l)*g(k, l) <=>$$
$$G(m, n)H_1(m, n) + g(-m, n)H_2(m, n) +$$
$$g(-m, n)H_3(m, n) + g(m, -n)H_4(m, n) \quad (37)$$

where

$$H_1(m, n) =$$
$$\frac{1}{4}[H(m, n) + H(-m, n) + H(m, -n) + H(-m, n)] \quad (38)$$

$$H_2(m, n) =$$
$$\frac{1}{4}[H(m, n) + H(-m, n) + H(m, -n) + H(-m, n)] \quad (39)$$

$$H_3(m, n) =$$
$$\frac{1}{4}[H(m, n) + H(-m, -n) + H(m, -n) + H(-m, n)] \quad (40)$$

$$H_4(m, n) =$$
$$\frac{1}{4}[H(m, n) + H(-m, n) + H(-m, n) + H(-m, n)] \quad (41)$$

If one of the convolved function, say h(k, l), is even, the convolution theorem simplifies to

$$h(k, l)*g(k, l) <=> H(m, n)G(m, n) \quad (42)$$

(f) cross correlation

$$h(k, l) \otimes g(k, l) <=>$$
$$G(m, n)H_1(m, n) + G(-m, -n)H_2(m, n)$$
$$-G(-m, n)H_3(m, n) - G(m, n)H_4(m, n) \quad (43)$$

if g(k, l) is even function, then

$$h_c(k, l)\, g(k, l) <=> G(m, n)\, H(m, n) \quad (44)$$

(g) DC value

$$H(0, 0) = \frac{T_x T_y}{MN} \sum_{k=0}^{M-1} \sum_{l=0}^{N-1} h(k, l) = T_x T_y \mu sybh \quad (45)$$

$$h(0, 0) = \frac{1}{T_x Tsuby} \sum_{k=0}^{M-1} \sum_{l=0}^{N-1} H(m, m) = (m, n) \quad (46)$$

(h) the quadratic content theorem

$$\frac{T_x T_y}{MN} \sum_{k=0}^{M-1} \sum_{l=0}^{N-1} [h(k, l)]^2 = \frac{1}{T_x T_y} \sum_{k=0}^{M-1} \sum_{l=0}^{N-1} [H(m, n)]^2 \quad (47)$$

The proof of (e) and (f) can be easily obtained using the following properties of the cas-function:

$$cas(x + y) = casx\ casy + cas(-x)sin\ y \quad (48)$$

$$cas(x + y) = casx\ casy + cas(-x)sin\ y \quad (49)$$

3.3.4 Computation of the Residual Geoid Undulation via the FHT

Using rectangular coordinates and in planar approximation, the residual geoid undulations $N_{\Delta g}$ computed from Δg's in an area E can be expressed by the following two-dimensional convolution integral:

$$N(x_p, y_p) = \frac{1}{2\pi\gamma} \iint_E \Delta g(x, y) \frac{1}{\sqrt{(x_p - x)^2 + (y_p - y)^2}} dxdy \quad (50)$$

If the given discrete gravity anomalies Δg are gridded point values, the residual geoid undulations $N_{\Delta g}$ at node (m, n) can be computed by

$$N(m, n) = \frac{1}{2\pi\gamma} \Delta g(m, n) * l_N(m, n) \quad (51)$$

$$l_N(m, n) = \Delta x \Delta y (x^2(m, n) + y^2(m, n))^{-1/2} \quad (52)$$

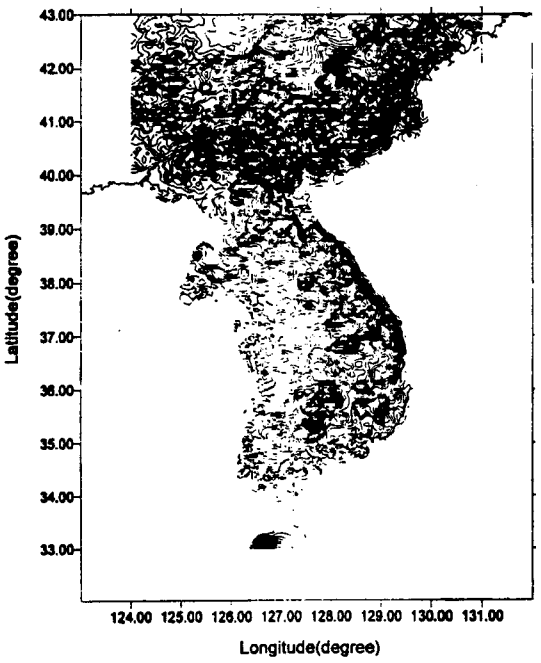

Fig. 4. Topography extracted from GTOPO40

Making use of the discrete Hartley transform, equation (35) can be efficiently evaluated by

$$N = \frac{1}{2\pi\gamma} H^{-1}\{\Delta G L_N\} \tag{53}$$

where ΔG and L_N are the discrete Hartley transforms of Δg and l_N respectively

$$\Delta G = H\{\Delta g\} \tag{54}$$

$$L_N = H\{l_N\} \tag{55}$$

If gravity anomalies are mean values, the kernel function l_N should be (Sideris and Li, 1992a and b).

$$l_N(m, n) = x \ln(y+\sqrt{x^2+y^2}) + y \ln(x+\sqrt{x^2+y^2}) \Big|_{(m-0.5)\Delta x}^{(m+0.5)\Delta x} \Big|_{(n-0.5)\Delta y}^{(n+0.5)\Delta y} \tag{56}$$

The observed gravity data (2,572 points) used is supplied by the National Geography Institute (NGI), Prof. Choi, K. S. in Pusan University, and Bureau Gravimetrique International (BGI) as shown in Fig. 5. Data were received in two basic forms: paper and digital listings. The raw data obtained is filtered to delete duplicate or obviously wrong data. These digital data were reformatted and corrected to the required processing parameters and datum used in this study. Gravity anomalies in the ocean area are based on a combination of Geosat, ERS-1 and Topex/Poseidon databases developed at BGI.

Especially, regression interpolation was applied to estimate gravity anomalies for the northern part of the Korean peninsula. Regression analysis is based on correlation between gravity anomalies and height. The following linear function was used

$$\Delta g_i = a + b \log H + v \tag{57}$$

Using GTOPO30 global digital elevation model resulting from a collaborative effort led by the staff at the US Geological Survey's EROS Data Center, 5'×5' regridded heights as shown in Fig. 4 were prepared for the northern area of the peninsula. Based on point free-air gravity anomalies and heights in the southern part, coefficients a and b of linear function are determined by least square method and linear regression equation is given

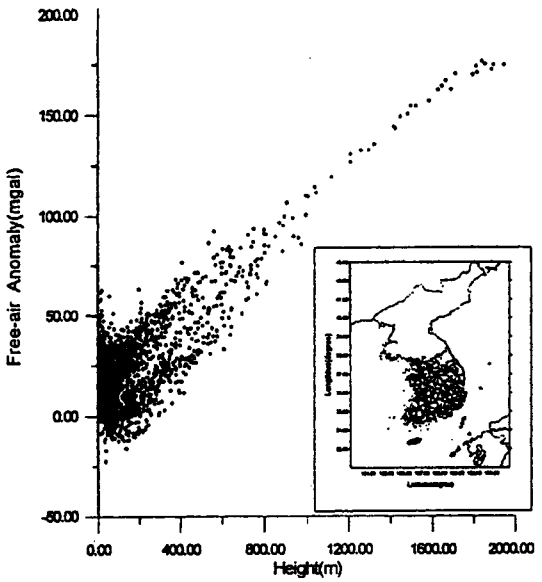

Fig. 5. The correlation between free-air gravity anomaly and height in the southern part of the Korean peninsula

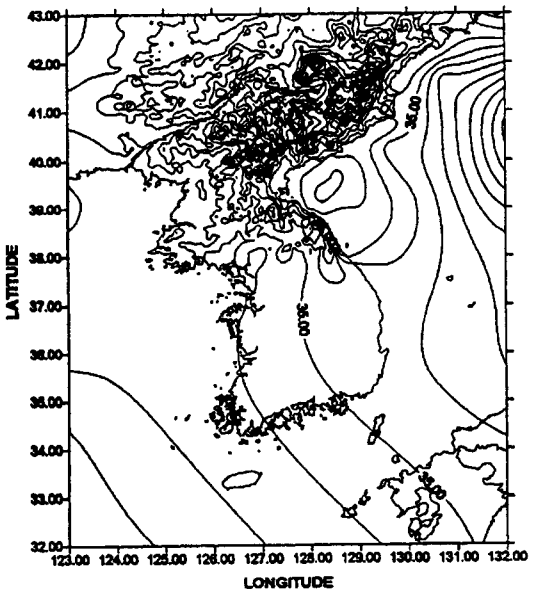

Fig. 6. Free-air gravity anomaly map obtained by regression in the northern area of the Korean peninsula. Contour Interval: 20 mGal

Table 1. Statistics of gravity anomalies and geoid undulations

Geopotential Model		MAX.	MIN.	MEAN	RMS	STD
OSU91A	N(m)	35.17	10.30	24.19	24.78	5.40
	Δg(mGal)	85.72	-95.14	16.41	24.03	17.55
EGM96	N(m)	33.68	8.18	23.68	24.28	5.38
	Δg(mGal)	107.97	-110.24	18.61	28.04	20.97
Free-air anomalies		246.93	-101.20	16.61	21.20	27.58
Residual anomalies		195.34	-57.19	4.45	17.32	19.71

$$\Delta g = 9.67 + 0.084 \log H \qquad (58)$$

Fig. 5 shows correlation of free-air anomaly and height, and gravity anomalies estimated in the northern area of the peninsula are shown in Fig. 6.

Pre-processing for geoid computation was to calculate the residual gravity anomalies. These residual anomalies were obtained by simply subtracting interpolated long wavelength effect from condensed gravity anomalies referred to a gravity formula corresponding to GR80. Because the use of local 5'×5' gravity data improves results significantly (Yun, 1995), the residual gravity anomalies were gridded in a grid span of 5'× 5' in the following area: $32^\circ \le \varphi \le 43^\circ$; $123^\circ \le \lambda \le 132^\circ$ by means of minimum curvature splines.

Fig. 7 shows the residual gravity anomalies. Statistics of all available data are summarized in Table 1. In order to compute the residual geoid undulations, field transformation technique used here is 2-D Fast Hartley Transform technique. The Hartley transform is superior to the Fourier transform with respect to requirements in both computer time and computer memory. The Hartley transformation is symmetric according to transformation formula and real signal is also real. These properties have led to the use of the

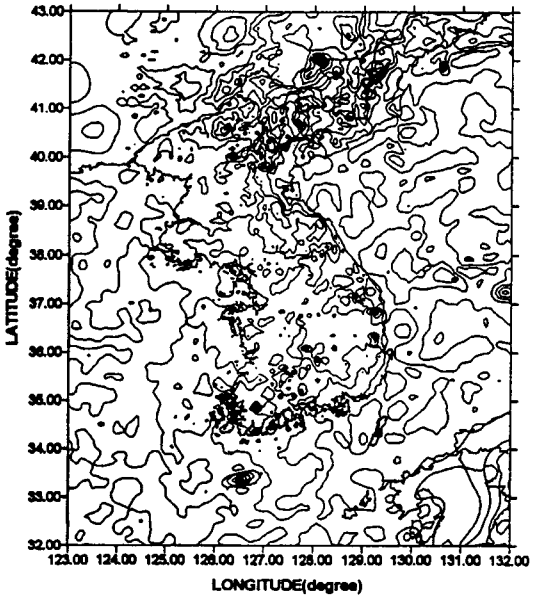

Fig. 7. Residual gravity anomalies from geopotential model minus Faye gravity anomaly. Contour Interval: 20 mGal

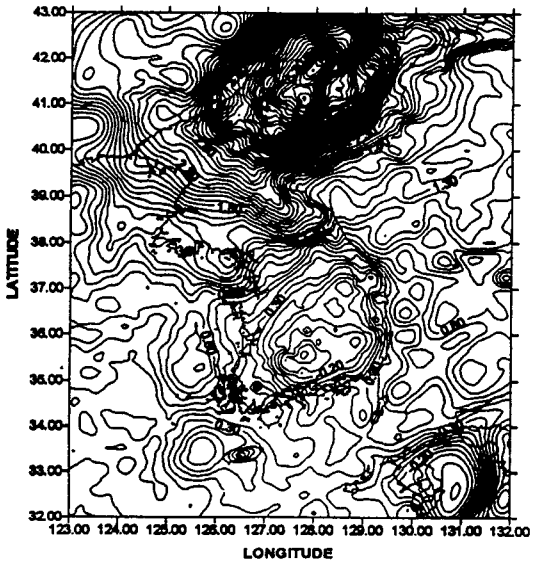

Fig. 8. Residual geoid undulations obtained from 2-D FHT with at least 100% zero-padding. Contour Interval: 10 cm

Hartley transform for time-efficient Fourier analysis of real signals. For a data length N being an integer power of 2, i.e, $N=2^n$, the FHT algorithm can be developed in just the same way as the FFT algorithm. As the FHT uses only real operations, it is about twice as fast as the FFT (Li, 1992).

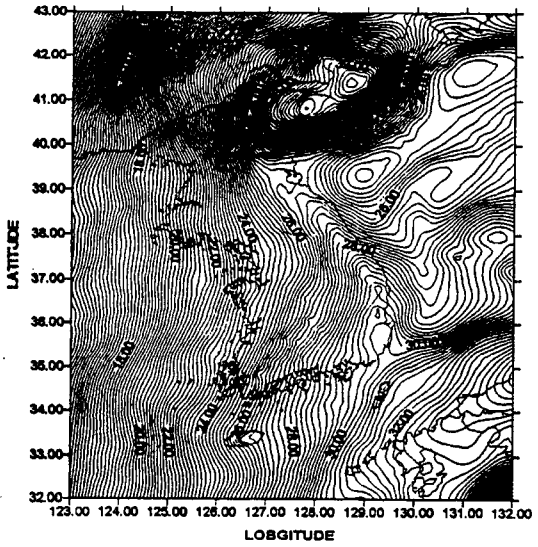

Fig. 9. The resulting geoid map based on EGM96 geopotential model by means of 2-D FHT with 100% zero-padding technique. Contour Interval: 20 cm

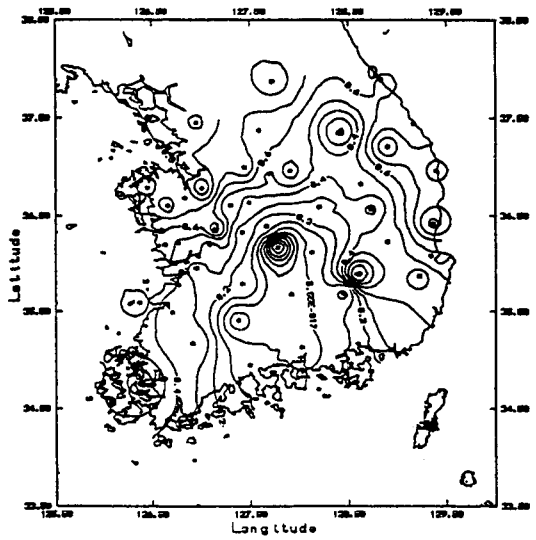

Fig. 10. Differences between the gravimetrc geoid solution and GPS/Leveling geoid. Contour Interval: 10 cm

To eliminate the effect of circular convolution on the computation, zero-padding was applied to each row and column of two data arrays. Fig. 8 shows the residual geoid undulation computed by FHT. The results shows larger value than that was given by Yun (1995) and Lee et al. (1996) It is clearly shown large differences is given by filling of empty cells in the northern area of peninsula.

Final geoid undulation was obtained by adding two effects. Fig. 9 shows final geoid surface referred to the GRS80 ellipsoid. The resulting geoid shows that difference is about 14 m from north-west to south-east side on land. For evaluating of the resulting quasi-geoid and for the determination of the geometric geoid, 49 GPS/ Leveling stations were used. The differences between two solutions, gravimetric geoid undulations are estimated to have an absolute accuracy close to 0.33 cm in the southern area of the peninsula. Although such evaluation in the northern area is not carried out, we consider that accuracy of result obtained from estimated gravity anomalies is improved.

4. Conclusions

In this study a gravimetric geoid solution was determined in and around the Korean peninsula using all available gravity. This involved EGM96 to degree and order 360 as reference geopotential model, and 2 dimensional Fast Hartley Transform. The Fast Hartley Transform is superior to the Fast Fourier Transform for the computations of real discrete convolutions, because in adding to having all advantages of FHT can save half of computer core compared with FFT.

To evaluate the resulting geoid, differences between gravimetric solution and GPS/Leveling were evaluated. Standard deviation versus maximum values of contribution from condensed

gravity anomalies is 1.06 vs. 1.55 meters. The geoid shows that difference from the north-west to the east south is about 14 meters across the Korean peninsula. From the comparison of gravimetric geoid and differences show up in hilly mountainous areas, suggesting that orthometric heights obtained from spirit leveling have a large error in mountainous areas.

References

1. Bold, G. E. J., "A Comparison of the Time involved in Computing Fast Hartley and Fast Fourier Transforms", *Proceedings of the IEEE,* **73**(12), 1985, 1863-1864.
2. Bracewell, R. N., "The fast Hartley Transform", *Proceedings of the IEEE,* **72**(8), 1984, 1010-1018.
3. Bracewell, R. N., "The Fourier Transform and its Application", Second edition, revised, McGraw-Hill, New-York., 1986.
4. Bracewell, R. N., O. Buneman and H. Hao, "Fast Two-dimensional Hartley Transform", *Proceedings of the IEEE,* **74**(9), 1986, 1282-1283.
5. Hartley, R.V.L., "A More Symmetrical Fourier Analysis Applied to Transmission Problems", *Proceddings of I. R. E.*, 1942, 144-150.
6. Lee, S. B., H. S. Yun and J. H. Choi, "Gravimetric Geoid Determination by Fast Fourier Transform in and Around Korean Peninsula", Journal of the Korean Society of Geodesy, Photogrammetry, and Cartography, **14**(1), 1996, 49-58.
7. Lee, S. Y., "Estimation of Gravity Anomalies and Geoid Determination in the Korean Peninsula", MSc. thesis, Department of Civil Engineering, Sung Kyun Kwan University, 1997.
8. Li, Y. C. and M. G. Sideris, "The fast Hartley Transform and its Application in Physical Geodesy", *Manuscripta Geodetica,* **17**, 1992, 381-387.
9. Li, Y. C., "Optimized spectral geoid determination", UCGE Rept. 20050, Dept. of Geomatics Engineering, The University of Calgary, Canada, 1993.
10. Schwarz et al., "Orthometric heights without leveling", *Journal of surveying Engineering,* **113**(1), 1987, 28-40.
11. Tziavos, I. A., "Numerical Considerations of FFT Methods in Gravity Field Modeling", Nr. 188, Hannover, 1993.
12. Vanicek, P. and N. T. Christou, "Geoid and Its Geographysical Interpretations", CRC Press, 1994, 77-93.
13. Yun, H. S. and J. Adam, "On the Global Geopotential Models in the Region of the Korean peninsula", Journal of the Korean Society of Geodesy, Photogrammetry, and Cartography, **13**(1), 1994.
14. Yun, H. S.(1995), "Results of the Geoid Computation for the Korean Peninsula", PhD. Dissertation, Technical University of Budapest, Hungary.